Further Advances of the Lippmann-Schwinger-Lanczos Algorithm for SAR Imaging in Presence of Multiple Scattering and Losses

Vladimir Druskin (WPI, SMU and BAAI), Mikhail Zaslavskiy (SMU)

Acknowledgments

Contributors:

- **Thomas Hagstrom**, Southern Methodist University
- **Shari Moskow**, Drexel University
- **Jörn Zimmerling**, Uppsala University

Partial support:

- Druskin: AFOSR grants FA 955020-1-0079, FA9550-23-1-0220, and NSF grant DMS-2110773.
- Zaslavskiy: AFOSR grant FA9550-23-1-0220.

1D inverse wave problem

- For simplicity consider a plane wave 1D problem on $[0, \infty]$,

$$-c^2(z)\frac{\partial^2}{\partial z^2}w(z,t) + \frac{\partial^2}{\partial t^2}w(z,t) = g_t(t)\delta(z - 0_+),$$

  with proper homogeneous initial and boundary conditions where $c(z) > 0$ is variable wave-speed, $g(t)$ is a (possibly narrow band) radar excitation.

- Transforming to travel-time coordinate $dx = \frac{dz}{c(z)}$ and using the Liouville transform we obtain the "plasma wave equation"

$$-\frac{\partial^2}{\partial x^2}u(x,t) + q(x)u(x,t) + \frac{\partial^2}{\partial t^2}u(x,t) = g_t(t)\delta(x - 0_+),$$

  $q = \frac{\frac{d^2}{dx^2}\sqrt{c(x)}}{\sqrt{c(x)}}$ is "reflectivity" of the media, i.e., $q = 0$ in absence of reflectors.

- Inverse problem: $u(0,t) \mapsto q(x)$.

Lippmann-Schwinger nonlinear formulation

- Consider also background solution $\mathbf{u}_0$

$$-\frac{\partial^2}{\partial x^2}u_0(x,t)+q_0(x)u_0(x,t)+\frac{\partial^2}{\partial t^2}u_0(x,t)=g(t)\delta(x-0_+)$$

.

- Convolving the background solution with the internal solution we arrive at the Lippmann-Schwinger (LS) integral equation

$$u(0,t)-u_0(0,t)=-\int_0^\infty\int_0^t\frac{d}{ds}u_0(x,t-s)\frac{d}{ds}u(x,s)(q(x)-q_0(x))\,dx\,ds$$

- Given $u(0,t)$ the LS become nonlinear integral equation with respect to $q(x)$

Lippmann-Schwinger-Lanczos (LSL)

- Assuming *we have an estimate* of the internal solution

$$u_{approx}(x,t) \approx u(x,t)$$

we reduce the nonlinear LS inverse IE to linear IE with respect to $q(\mathbf{r})$

$$u(0,t) - u_0(0,t) = -\int_0^\infty \int_0^t \frac{d}{ds} u_{approx}(x,t-s) \frac{d}{ds} u_0(x,s)(q(x) - q_0(x))$$

- Born approximation

$$u_{approx} = u_0(x,t)$$

- The LSL uses a more accurate estimate u_{approx} computed via a data-driven nonlinear transform from $u_0(x,t)$.

Prior data-driven ROM and LSL developments

- Data-driven reduced order model (ROM) for wave imaging [Dr.,Mamonov, Zaslavskiy, Thaler, 2016; Dr.,Mamonov Zaslavkiy, 2018; Borcea, Dr., Mamonov, Zaslavskiy, 2019, 2020; Borcea, Garnier, Mamonov, Zimmerling, 2023,2024]
- Computation of data-driven internal solutions [Borcea, Dr., Moskow, Mamonov, Zaslavkiy, 2020]
- LSL in frequency and time domain [Dr., Moskow, Zaslavkiy, 2021, 2022, 2024]
- LSL imaging with SAR-to-MIMO data completion (lifting) [Dr., Moskow, Zaslavkiy, 2024]
- Layered media with propagation and losses, optimal grid inversion [Borcea, Dr, Zimmerling, 2021].

2024 developments, in this talk

1. Foundation of data-driven internal solutions: ROM theory of transmutation matrices.
2. Incorporation of sparse inversion, application to narrow bound pulses;
3. Application to 3D synthetic models
4. Extension of the LSL to simultaneous determination of the impedance and loss profiles

Marchenko-Gelfand-Levitan transmutation operators

- Let $u(x,t)$ is the internal solution for unknown $q(x)$ and $u_0(x,t)$ is the background solution for $q_0(x)=0$. Then Marchenko-Gelfand-Levitan theory gives

$$u(x,t)=\int_0^t T(t,t')u_0(x,t')dt,$$

where $T(t,t)$ is data-driven Volterra transmutation operator Kernel [Marchenko, Gelfand, Levitan, 1950s]

- Discrete transmutation [Bube, Burridge, 1983; Natterer, 1989]:

$$\mathbf{U}_{approx}=\mathbf{U}_0\mathbf{T}$$

$\mathbf{U}_{approx}=[u_{approx}(x,0),u_{approx}(x,\tau),\dots,u_{approx}(x,(m-1)\tau)]$,
$\mathbf{U}_0=[u_0(x,0),u_0(x,\tau),\dots,u_0(x,(m-1)\tau)]$,
$\mathbf{T}\in\mathbb{R}^{m\times m}$ is upper triangular.

- Exactness for a specially chosen class of piecewise-constant media [Bube, Burridge 1983; Borcea et al, 2024].

Operator initial-value problem

- Denote symmetrized solution $\mathbf{u}(x,t) = \frac{u(x,t)+u(x,-t)}{2}$, for practical purposes $\mathbf{u}(x,t) \approx u(x,t)$
  Then [1]

$$\mathbf{A}\mathbf{u}(x,t) + \frac{d^2}{dt^2}\mathbf{u}(x,t) = 0, \ \mathbf{u}(t=0) = \mathbf{b}(x), \ \frac{d}{dt}u(t=0) = 0$$

  where $\mathbf{A}\mathbf{u}(x) = -\frac{d^2}{dx^2}\mathbf{u}(x) + q(x)\mathbf{u}(x)$.
- Representation via function of the operator:

$$\mathbf{u}(x,t) = \cos(t\sqrt{\mathbf{A}})\mathbf{b}(x).$$

[1] Dr., Mamonov, Thaler, Zasl. 2016

Data sampling and Gramian of data-driven ROM

- Assume that $\mathbf{u}(0,t)$ is discretized with sampling rate τ (consistent with Nyquist frequency of $g(t)$). We want to estimate the unknown internal solutions $\mathbf{u}(x,t_k) = \cos(k\tau\sqrt{\mathbf{A}})\mathbf{b}$ for $x > 0$, $k = 0,\dots,n-1$ from data $\mathbf{u}(0,j\tau)$, $j = 0,\dots,2n-1$.
- Denote $L_2[0,\infty]$ inner product $\langle u(x); v(x)\rangle = \int_0^\infty u(x)v(x)dx$
- Let $\mathbf{M} \in \mathbb{R}^{n\times n}$ is the Gramian of the internal snapshots. *The Gramian completely defines the ROM of the wave propagation that reproduces* $\mathbf{u}(0,j\tau)$, $j = 0,\dots,2n-1$. $\mathbf{M}$'s elements are given by

$$\mathbf{M}_{kl} = \langle \mathbf{u}(t_k); \mathbf{u}(t_l)\rangle = \langle \cos(k\tau\sqrt{\mathbf{A}})\mathbf{b}; \cos(l\tau\sqrt{\mathbf{A}})\mathbf{b}\rangle =$$

$$\frac{1}{2}\langle \mathbf{b}; \cos((k+l)\tau\sqrt{\mathbf{A}})\mathbf{b}\rangle + \frac{1}{2}\langle \mathbf{b}; \cos((k-l)\tau\sqrt{\mathbf{A}})\mathbf{b}\rangle =$$

$$(\mathbf{u}[0,\tau(k+l)] + \mathbf{u}(0,\tau|k-l|))/2.$$

- Now we from the Gramian we estimate the projection of the true snapshots on the background ones using their causality.

Uniqueness of casual transmutation matrices

- Denote $\mathbf{M}_0$ the Gramian computed for the background (known) solution with $q_0(x) = 0$.

Theorem

The row vector of data-generated internal fields $\mathbf{U}_{approx} = \mathbf{U}_0 T$ *with upper triangular transmutation matrix* $\mathbf{T}$ *is uniquely defined by the data. The transmutation matrix is given by*

$$\mathbf{T} = (L_0^\top)^{-1} L^\top,$$

where upper triangular matrices L *and* L_0 *are defined via Cholesky factorizations*

$$\mathbf{M} = LL^\top \qquad \mathbf{M}_0 = L_0 L_0^\top$$

- The Cholesky factorization of $\mathbf{M}$ constitutes the nonlinear part of the data transform.

Optimal properties of data-generated internal solutions

- Assume $g(t) = \frac{\delta(t-\tau/2)+\delta(t+\tau/2)}{\tau}$, that yields the space of background solution $\mathbf{u}_0(x, i\tau)$ as the space of piecewise-constant functions with step τ. Denote $\mathbf{U}_{opt} = [u_{opt}(x,0), u_{opt}(x,\tau), \ldots, u_{opt}(x, i(m-1)\tau)]$ the $L_2[0,\infty]$ projection of $\mathbf{U}$ onto the space of the background solution.

Theorem

For reqular enough $q(x)$ and small $\|\mathbf{U} - \mathbf{U}_{opt}\|_{L_2}$

$$\|\mathbf{U}_{approx} - \mathbf{U}\|_{L_2[0,\infty]} = \|\mathbf{U} - \mathbf{U}_{opt}\|_{L_2[0,\infty]}[1 + o(1)].$$

- The analysis extendable to problems with band-limited pulses, multi-dimensional MIMO/SAR and losses, with possibly weaker results.

Sparsity-promoting regularization for narrow-band signals

- Lower resolution compared to wide-band signals
- Need to constrain the model to sparsely distributed scatterers
- L_1-penalty term or similar can be employed

Linear Born processing

True medium

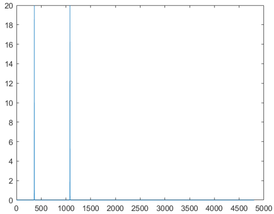

Linear Born processing

True medium

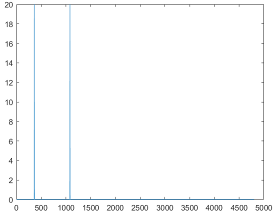

Born image

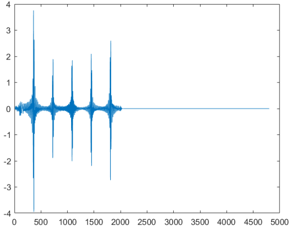

Scattered field for a highly modulated Gaussian pulse.

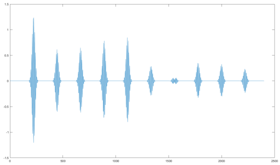

Linear Born processing

True medium

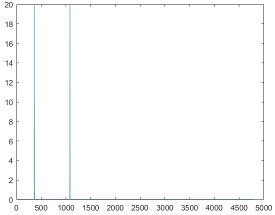

Born image

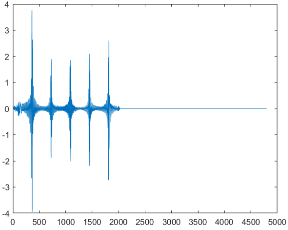

Scattered field for a highly modulated Gaussian pulse.

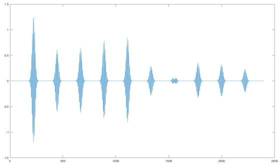

Low resolution, multiple scattering artifacts. Can we do better with conventional nonlinear data processing, e.g., sparsity promoting imaging?

Sparsity promoting nonlinear Born processing

True medium

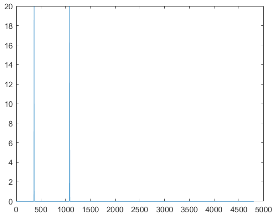

Sparsity promoting nonlinear Born processing

True medium

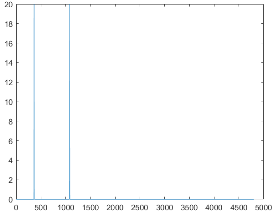

Born with SVD truncation (linear processing)

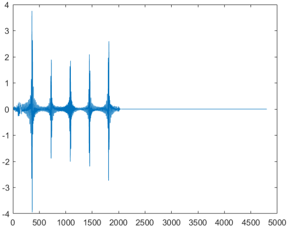

Born with L_1-penalty

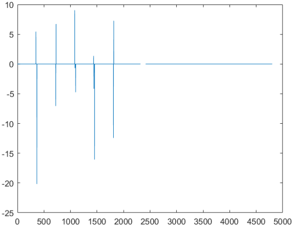

Sparsity promoting nonlinear Born processing

True medium

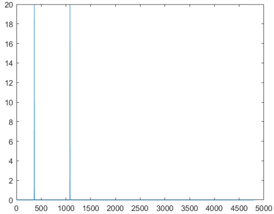

Born with SVD truncation (linear processing)

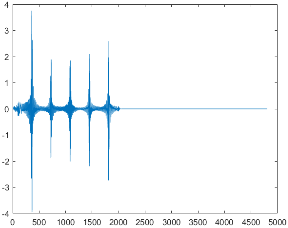

Born with L_1-penalty

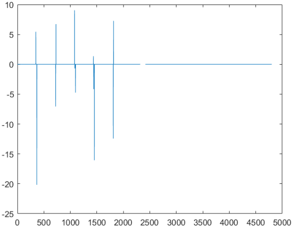

Better resolution but multi-scattering artifacts remain

Lippmann-Schwinger imaging using data-driven ROMs

True medium

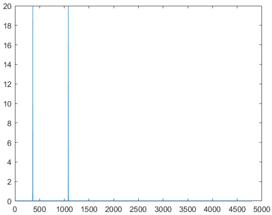

Lippmann-Schwinger imaging using data-driven ROMs

True medium

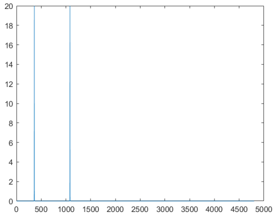

Cheated solution

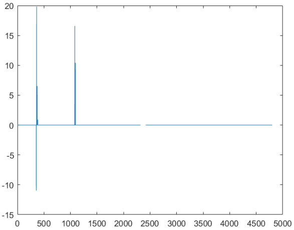

LS + ROM

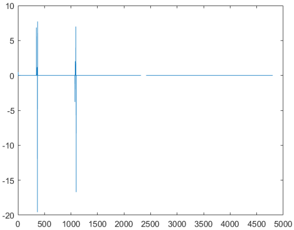

Lippmann-Schwinger imaging using data-driven ROMs

True medium

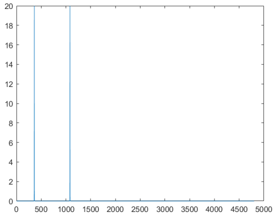

Cheated solution

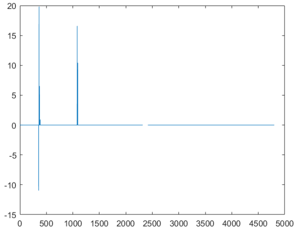

LS + ROM

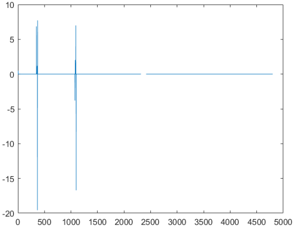

Born

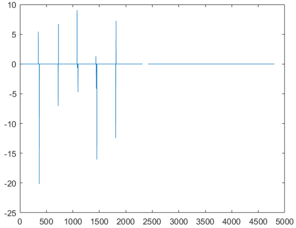

LASSO regularization for 2D problem

True medium

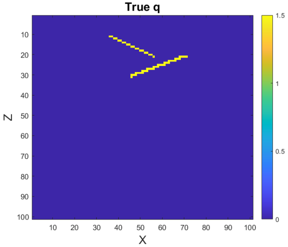

LASSO regularization for 2D problem

True medium

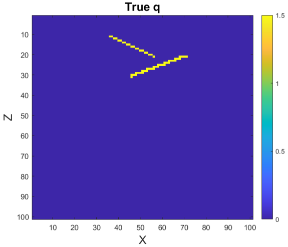

LSL+LASSO

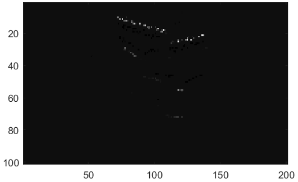

LASSO regularization for 2D problem

True medium

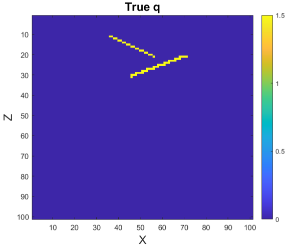

Born+LASSO

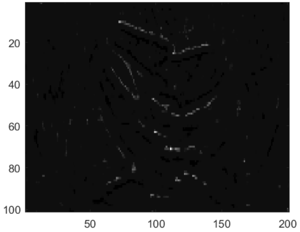

LSL+LASSO

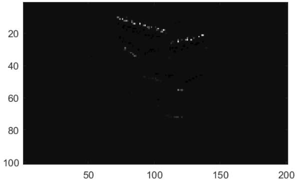

- Similar penalty term can be used in Born imaging
- Takes care of narrow-band signals
- Ghost images still stay in Born results

Cross-section imaging of 3D object

- 3D object (donut) in half-space
- Data is collected along a single trajectory
- Multiple bouncing between donut and ground
- Similar effects as in GOTCHA dataset

True model

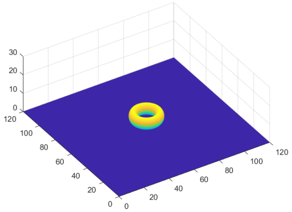

- Data is simulated using fast time-domain integral-equation-based solver to generate data (Barnett, Greengard, Hagstrom, 2019)
- 2D imaging in cross-section is viable solution

Imaging of 3D donut

True model

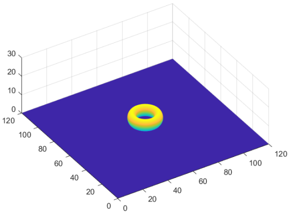

Born

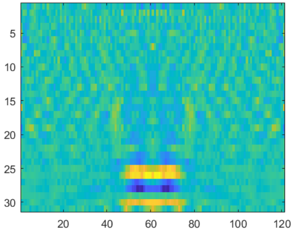

Imaging of 3D donut

True model

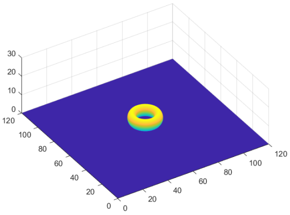

LSL

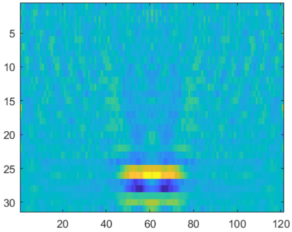

Born

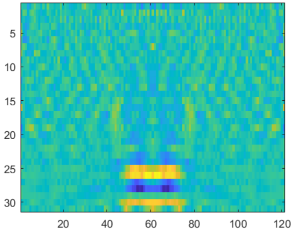

- Multiple bouncing artifact (yellow ghost image below the donut) is suppressed
- Quality can be hopefully improved by fully 3D imaging

Wave propagation in lossy medium in 1D

- First-order frequency-domain formulation in travel-time coordinates

$$\left(\begin{pmatrix} 0 & \partial_x \\ \partial_x & 0 \end{pmatrix} + \begin{pmatrix} r & \frac{1}{2}(log(\sigma))_x \\ -\frac{1}{2}(log(\sigma))_x & 0 \end{pmatrix} + i\omega I\right)\begin{pmatrix} u \\ v \end{pmatrix} = \frac{\hat{g}(\omega)}{i\omega}\delta(x)$$

- Data of given by $u(0,\omega_i),\ u'(0,\omega_i),\ i = 1,\dots,n$
- Lippmann-Schwinger integral equation" for $i = 1,\dots n$

$$u(0,\omega_i) - u_0(0,\omega_i) =$$

$$-\int_0^\infty \begin{pmatrix} u_0(x) \\ v_0(x) \end{pmatrix}^T \begin{pmatrix} r & \frac{1}{2}(log(\sigma))_x \\ -\frac{1}{2}(log(\sigma))_x & 0 \end{pmatrix} \begin{pmatrix} u(x) \\ -v(x) \end{pmatrix} dx.$$

- Given data $u(0,\omega_i),\ i = 1,\dots,n$, it is nonlinear integral equation with respect to losses r and impedance σ

Imaging in 1D lossy medium

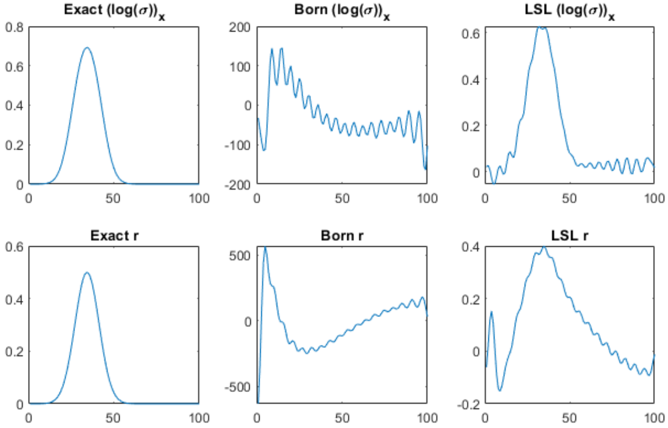

Conclusions

- Data-driven transmutation matrices allows to produce near best approximation of the internal solution in the subspace of the background solution, that can be treated as a finite-element subspace.
- The data-driven internal solutions suppress imaging artifacts due to multi-scattering and losses, as shown on 1D, 2D and 3D examples.
- Similarly to linear inversion, sparsity constraints improve resolution in our nonlinear framework, in particular for band-limited signals
- Current limitation: theoretical computational cost is comparable with Born inversion, however efficient implementation requires developing more efficient linear algebra. Work in progress.
- To-Do: Application to industry standard experimental data-sets (GOTCHA, etc.); Imaging though walls, vegetation, underground, including losses and dispersion in multiple dimensions.